NUCLEAR RESONANCE STUDIES OF ANTIFERROMAGNETIC CRYSTALS IN ZERO-FIELD

Thesis for the Degree of M. S.
MICHIGAN STATE UNIVERSITY

Doohee Kim

1962

NUCLEAR RESONANCE STUDIES OF ANTIFERROMAGNETIC CRYSTALS IN ZERO-FIELD

By

Doohee Kim

A THESIS

Submitted to
Michigan State University
in partial fulfillment of the requirements
for the degree of

MASTER OF SCIENCE

Department of Physics

1962

ACKNOWLEDGMENT

I wish to express my gratitude to Professor R. D. Spence for suggesting the topic and for his kind guidance throughout this work.

****

TABLE OF CONTENTS

I. INTRODUCTION

In the study of nuclear magnetic resonance of antiferromagnetic crystals, it is customary to find the direction of the local magnetic fields at probe nuclei sites in the presence of a large external magnetic field. This method is rather tedious, and a number of helium runs are required to complete the study of a single crystal. In addition to this, it has been shown that the external magnetic field perturbs the spin arrangement of the magnetic ions, and the results are not completely characteristic of the crystal itself. In view of these difficulties, we have examined an alternate method of finding the local magnetic field. It is the purpose of this thesis to show that nuclear magnetic resonance experiment in zero field (no external magnetic field) removes these difficulties.

II. THE THEORY AND THE TECHNIQUE OF THE METHOD

The apparatus used for the zero field method is the same as that for the applied field method except there is no magnet. In place of the magnet, one uses a modulation coil, by which a time varying magnetic field can be oriented in all directions. The set-up is shown in Figures 1 and 2.

The nuclear magnetic resonance occurs if the total magnetic field H_t; which the nucleus experiences, and the frequency of the detecting device satisfy the following relation.

(1) $h\nu = g\mu H_t$

where g: the g factor for the nucleus

μ: the nuclear magneton

H_t: the total magnetic field at the nuclear sites

h: Planck's constant

ν: the detector frequency

Here H_t consists of the internal field of the crystal at the nucleus sites and the modulation field. The total field is given by:

(2) $H_t^2 = H_l^2 + H_m^2 + 2\,\vec{H_l} \cdot \vec{H_m}$

where H_l is the local field and H_m is the modulation field.

If in an antiferromagnetic crystal there exists a set of proton sites which experience a given local magnetic field, there exist an equal number of proton sites which experience a local magnetic field of the same magnitude but of opposite direction. Thus the total field for these two cases is given by:

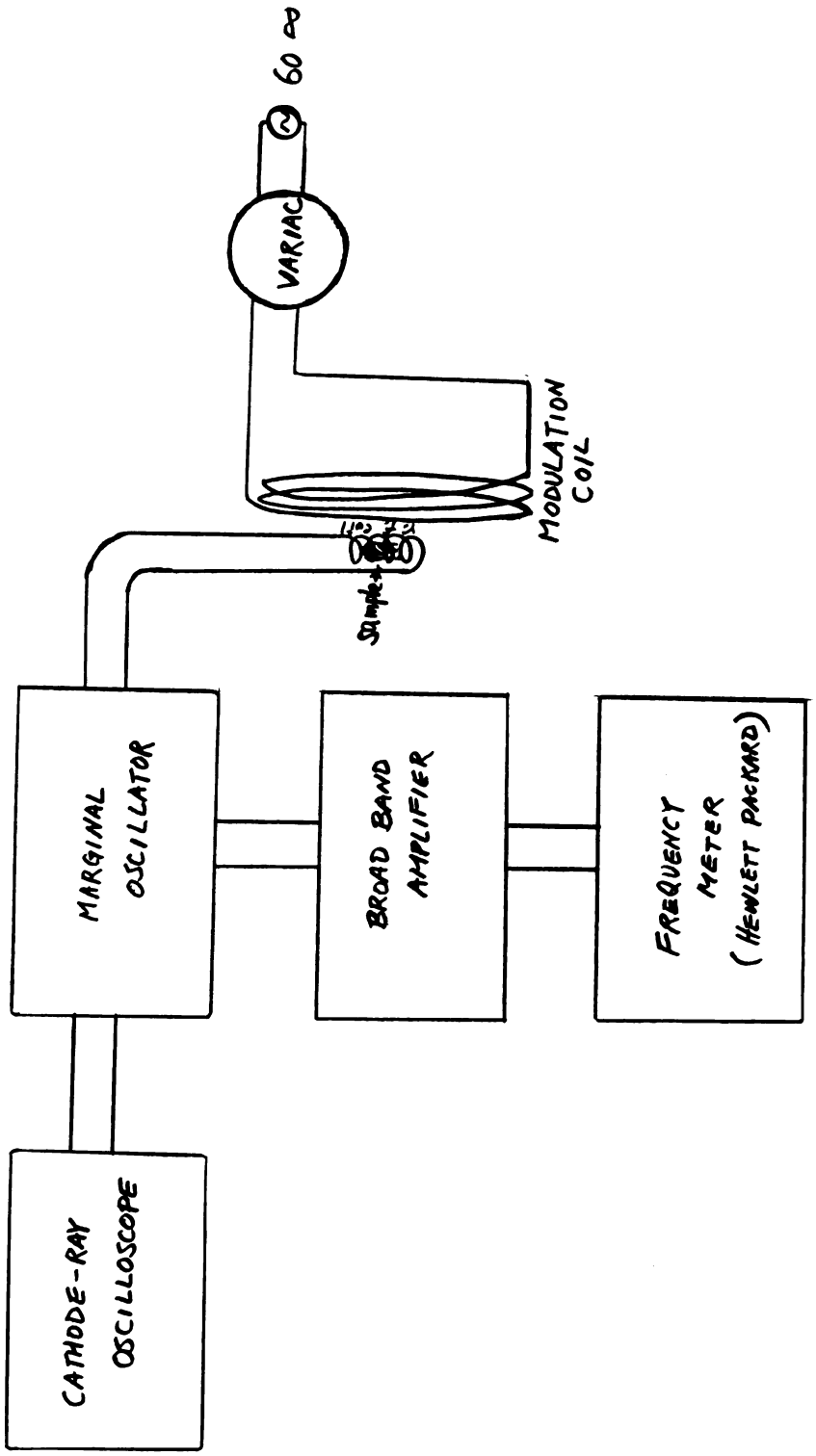

Figure 1. Block diagram of the zero-field set-up.

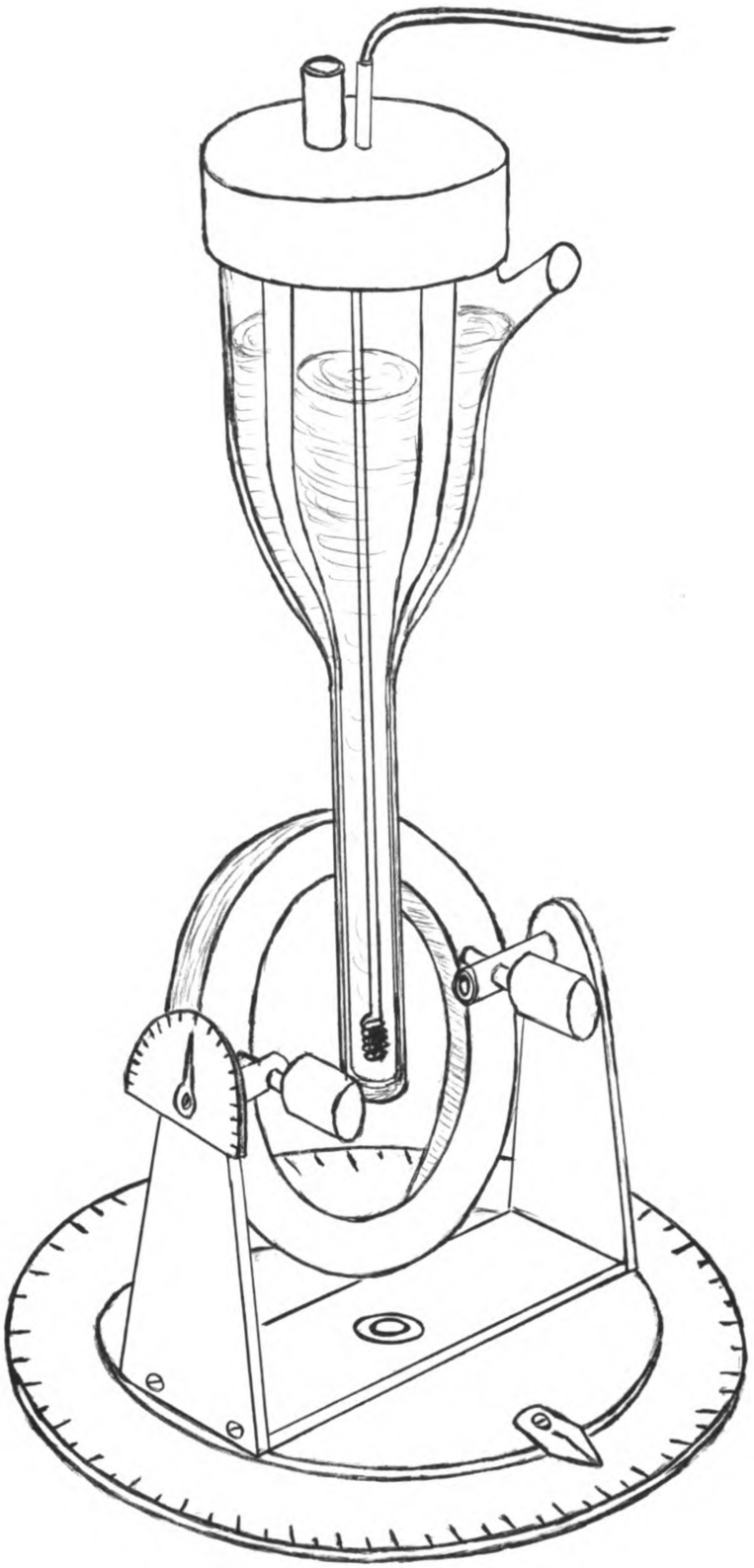

Figure 2. Modulation coil and the sample.

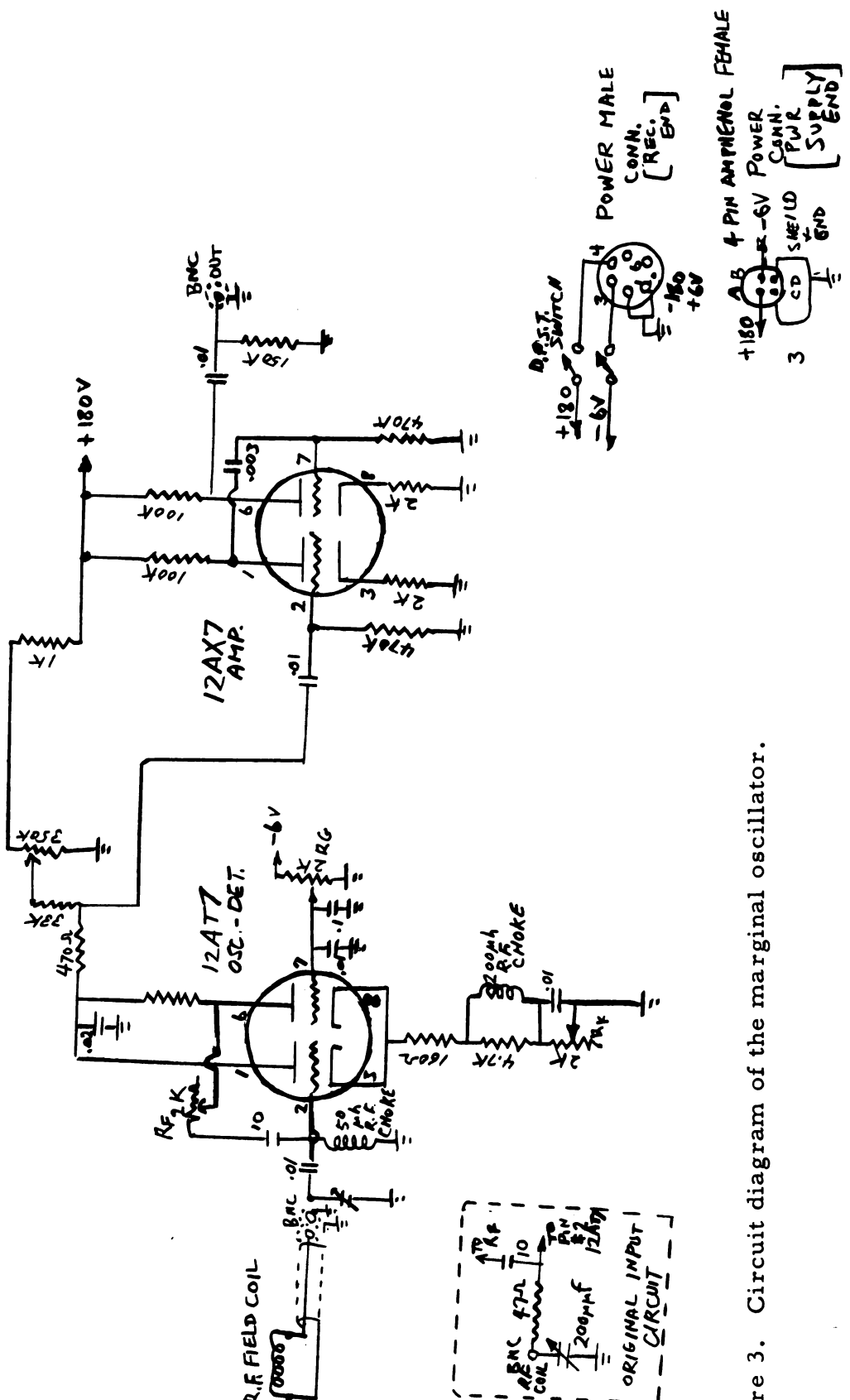

Figure 3. Circuit diagram of the marginal oscillator.

$$(2') \quad H_t^2 = H_1^2 + H_m^2 + 2|H_1|\,|H_m| \sin\theta \cos\phi$$

$$(3) \quad H_t^2 = H_1^2 + H_m^2 - 2|H_1|\,|H_m| \sin\theta \cos\phi$$

where H_m is along x-axis, and θ, ϕ the polar and azimuthal angle of one of the local field vectors respectively.

As the result of the time variation of the modulation field, the total magnetic field H_t fluctuates within the limits determined by the amplitude of the modulation. If, within these limits, the total magnetic field satisfies equation (1), the nuclei will absorb the power from the detector. Except for large modulation field, the absorption will occur at two places in the period of the modulation cycle.

If the absorption signals are viewed on the oscilloscope, which is synchronized to the modulation, resonance lines are observed when the following conditions are satisfied.

$$(4) \quad H_{mo}\sin(\omega_m t_1) = -|H_1 \sin\theta \cos\phi| + \sqrt{(H_1 \sin\theta \cos\phi)^2 + (H_t^2 - H_1^2)}$$

$$(5) \quad H_{mo}\sin(\omega_m t_2) = +|H_1 \sin\theta \cos\phi| - \sqrt{(H_1 \sin\theta \cos\phi)^2 + (H_t^2 - H_1^2)}$$

where ω_m is the modulation frequency, and H_{mo} is the modulation amplitude. With this definition of t_1 and t_2, the separation between the two signals is given by:

$$(6) \quad t_1 - t_2 = \frac{2}{\omega_m} \arcsin\left(\frac{-|H_1 \sin\theta \cos\phi| + \sqrt{(H_1 \sin\theta \cos\phi)^2 + (H_t^2 - H_1^2)}}{H_{mo}}\right)$$

Figure 4 shows the separation as a function of the orientation of the modulation field for $CoCl_2 \cdot 6H_2O$, where the solid line represents the calculated values and the circles the experimentally observed values.

The smallest separation occurs when the modulation field and the local field vectors are parallel; therefore, to determine the direction of the local magnetic field, it is sufficient to measure the separation as a function of the orientation of the modulation coil with respect to the sample-crystal.

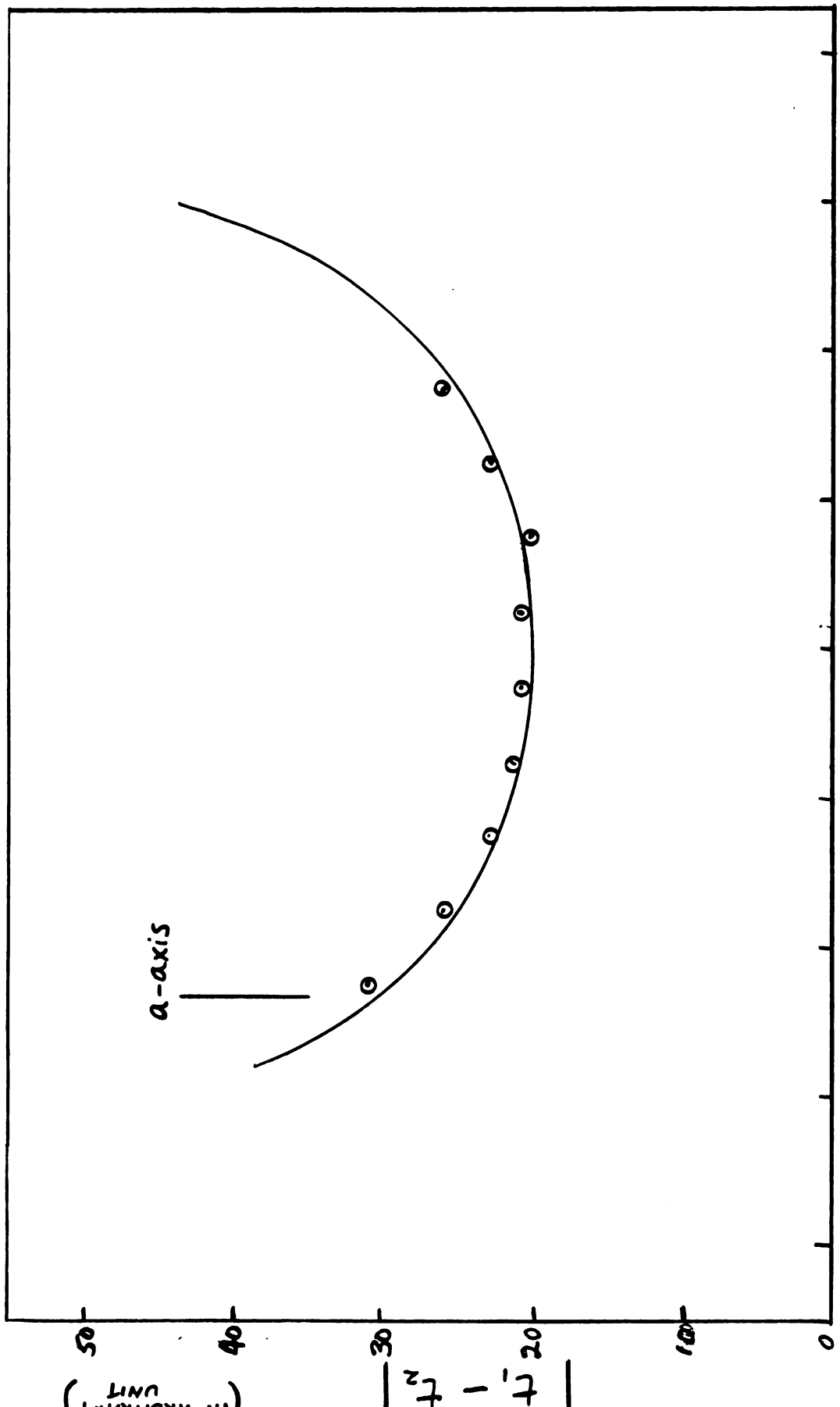

Figure 4. $|t_1 - t_2|$ vs. the direction of $\overrightarrow{H_m}$ as $\overrightarrow{H_m}$ is rotated around the b-axis of $CoCl_2 \cdot 6H_2O$ at 2.0^0K.

This can be done very rapidly by watching the separation of the two resonance lines on the oscilloscope, and this speed is one of the advantages of the method.

The magnitude of the local field is determined by setting the frequency of the detector so that the two signals coalesce at all orientations of the modulation field. The value of this frequency inserted to the equation (1) gives the magnitude of the local field.

The detecting system consists of the marginal oscillator, modulation coil, oscilloscope, and the frequency counter. The circuit diagram of the marginal oscillator is shown in Figure 3. In order that the Hewlett Packard frequency meter respond to the small power output of the oscillator it is necessary first to amplify it through a broad band amplifier.

To achieve all possible orientations of the modulation field, the field must be generated by a single coil with the crystal displaced from its center. The modulation field this arrangement produces at the sample is not very uniform in magnitude or direction.

For the modulation coil geometry and crystal size used in these experiments, the modulation amplitude varies by 5% and the direction of the modulation field varies by $\pm 3^{\circ}$ over the sample. The amplitude of modulation was about 50 gauss with the variac setting at 70 v. Since the natural line width is the order of 5 gauss, the broadening effect of the resonance line due to the modulation amplitude spread can be reduced by using a small modulation amplitude.

Thus the zero-field method has two advantages over the applied field method; namely, the rapidity in finding the local field vectors and the negligible distortion of the magnetic moments.

III. APPLICATIONS

In this section, we examine some of the information obtained from antiferromagnetic crystals by using the zero field method. Oscilloscope pictures of the proton resonance of typical antiferromagnetic crystals in zero-field are shown in Figure A to Figure G.

Analysis of our zero field study of $CuCl_2 \cdot 2H_2O$ shows that there are eight local fields, all having the same magnitude but different directions. Each signal arising from these fields is split into two components by the dipole-dipole interaction of protons in the same water molecule. Within experimental error, the results are in agreement with those of the Leiden group [2].*

The interaction potential V_{12} of two magnetic dipoles is given by:

$$(7) \qquad V_{12} \simeq \frac{\vec{\mu}_1 \cdot \vec{\mu}_2}{r_{12}^3} - \frac{3(\vec{\mu}_1 \cdot \vec{r}_{12})(\vec{\mu}_2 \cdot \vec{r}_{12})}{r_{12}^5}$$

where $\vec{r}_{12}$ is the vector connecting two dipoles of moment $\vec{\mu}_1$ and $\vec{\mu}_2$.

In hydrated crystals, the distance between the protons in the same water molecule is shorter than that between protons in different water molecules. In most of the cases the distance is so much shorter that only the dipole-dipole interaction of protons in the same water is important, and in evaluating V_{12} one has only to consider such protons.

As a result of V_{12} the energy levels are distorted, with a consequent shift of the resonance frequencies, which is a function of the angle between the local magnetic field at the proton sites and the proton-proton direction.

---

*Numbers in brackets are reference numbers.

1. $CuCl_2 \cdot 2H_2O$

The resonance frequencies and the orientation of the local fields in $CuCl_2 \cdot 2H_2O$ are shown in Table 1. Here θ is the angle measured from the crystallographic c-axis and ϕ is measured in the a-b plane from the a-axis. The orientations are shown graphically in the stereogram of Figure 5.

Table 1.

The proton resonance frequency (MHz)		The direction of the local field		Temperature
		θ	ϕ	
ν_A^*	3.12	65°	37°	2.15°K
ν_B^*	3.04	65°	37°	

2. $NiCl_2 \cdot 6H_2O$

There are four local magnetic fields at the proton sites in this crystal below the Néel temperature (6.2°K). The highest and the lowest frequency resonance lines show the doublet-splitting but the intermediate frequency lines did not. Figure 6 and Table 2 show the results obtained at 4.2°K.

Table 2.

The local magnetic field vector at proton sites	The resonance frequency (MHz)	Temperature (°K)
A	6.39	4.2°K
B	5.17	
C	4.67	
D	3.18	

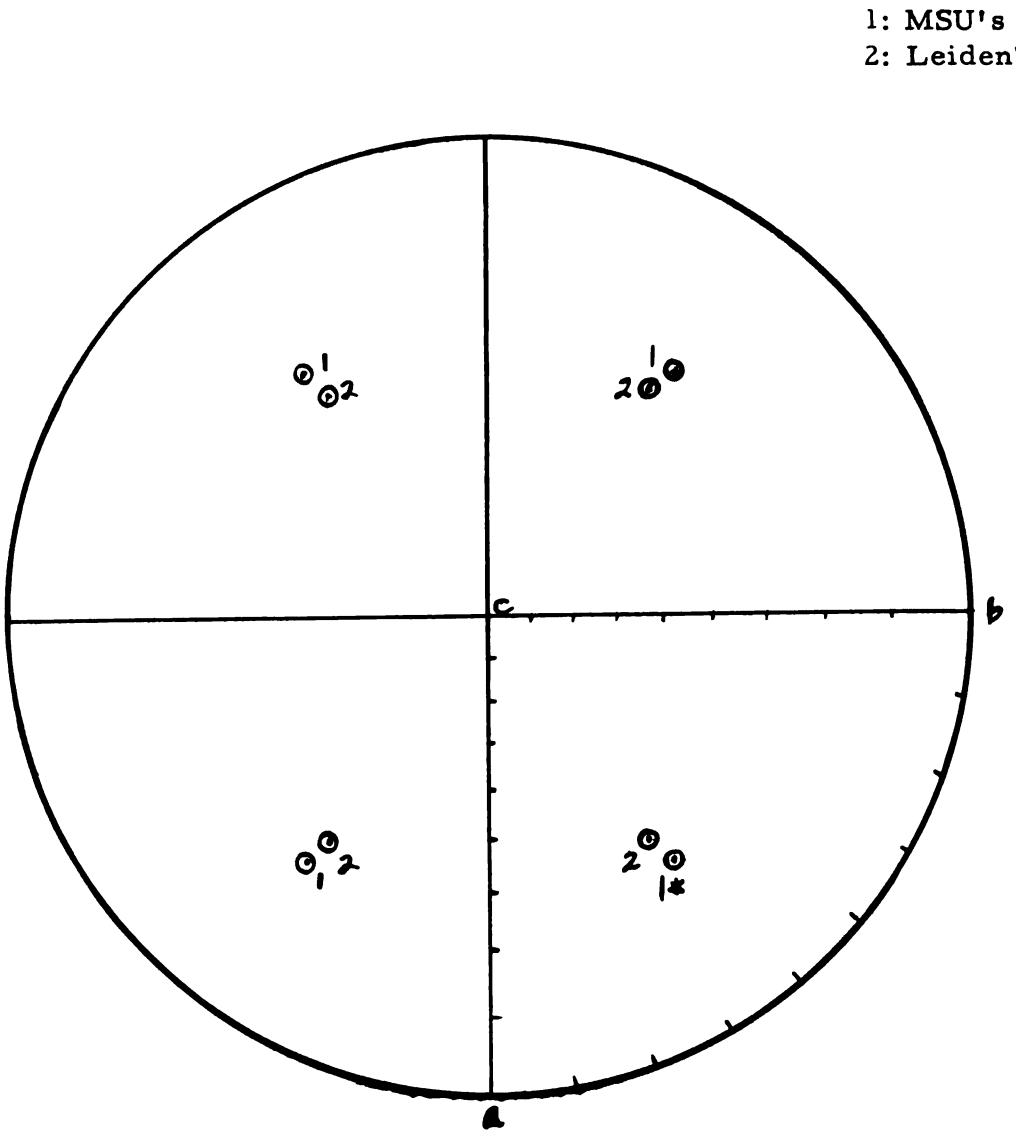

Figure 5. Stereographic projection of the local magnetic fields at the proton sites in $CuCl_2 \cdot 2H_2O$ (ours at 2.15°K).

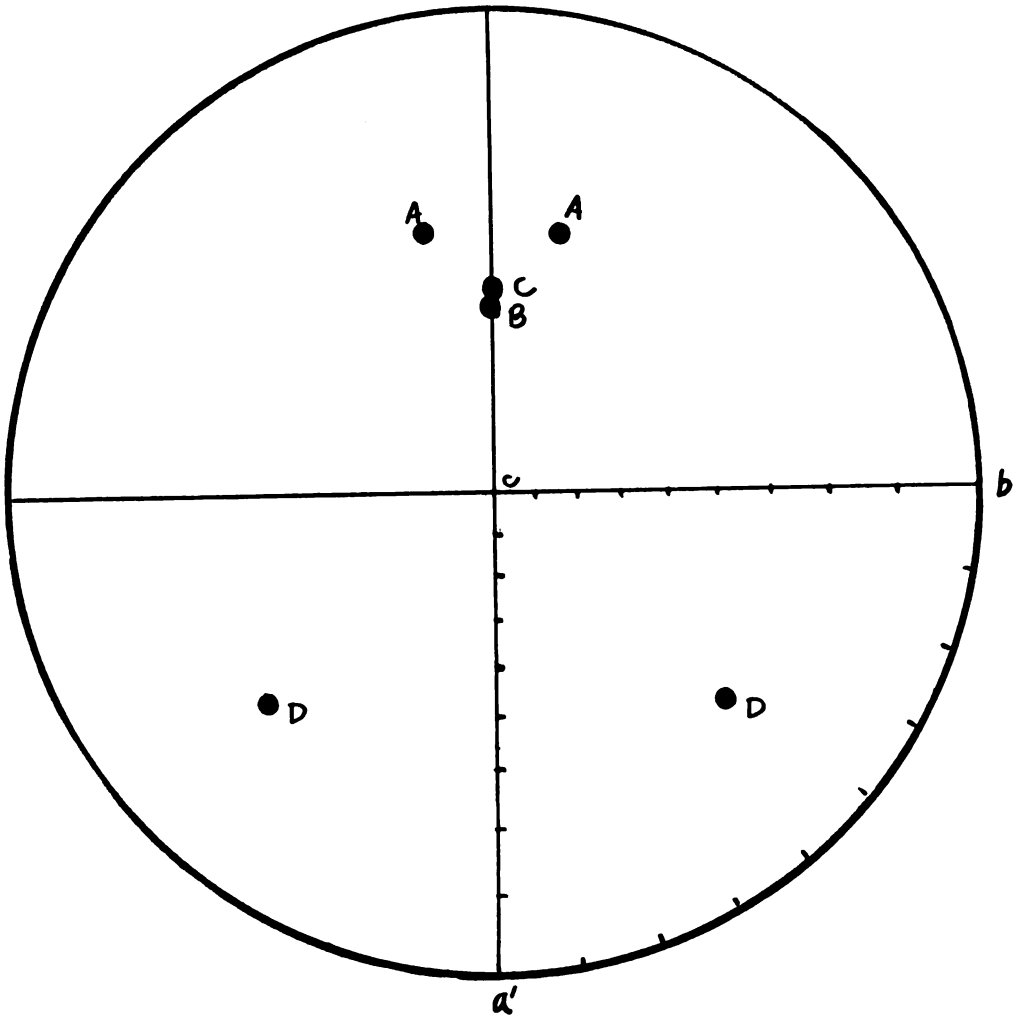

Figure 6. Stereographic projection of the local magnetic fields at the proton sites in $NiCl_2 \cdot 6H_2O$ at 4.2°K.

3. $CoBr_2 \cdot 6H_2O$

The numerical results of the local magnetic fields are given in Table 3.

Despite the fact that the crystals $CoCl_2 \cdot 6H_2O$ and $NiCl_2 \cdot 6H_2O$ are isostructural [3, 4], the $CoBr_2 \cdot 6H_2O$ and $NiCl_2 \cdot 6H_2O$ are quite different magnetically.

Table 3.

The local magnetic field vector at proton sites	The resonance frequency (MHz)	Temperature (^{o}K)
A	6.99	
B	5.80	2.5^{o}K
C	3.70	

4. $M_nCl_2 \cdot 4H_2O$

Three groups of proton resonance lines were observed for this crystal below the Néel temperature (1.62^{o}K). The local fields seem to lie all in the a'-b plane of the crystal as shown in Figure 7. The numerical results are given in Table 4.

Table 4.

The local magnetic field vector at proton sites	The resonance frequency (MHz)	Temperature (^{o}K)
A	8.1	
B_1	7.0	1.17^{o}K
B_2	7.0	
C	5.7	

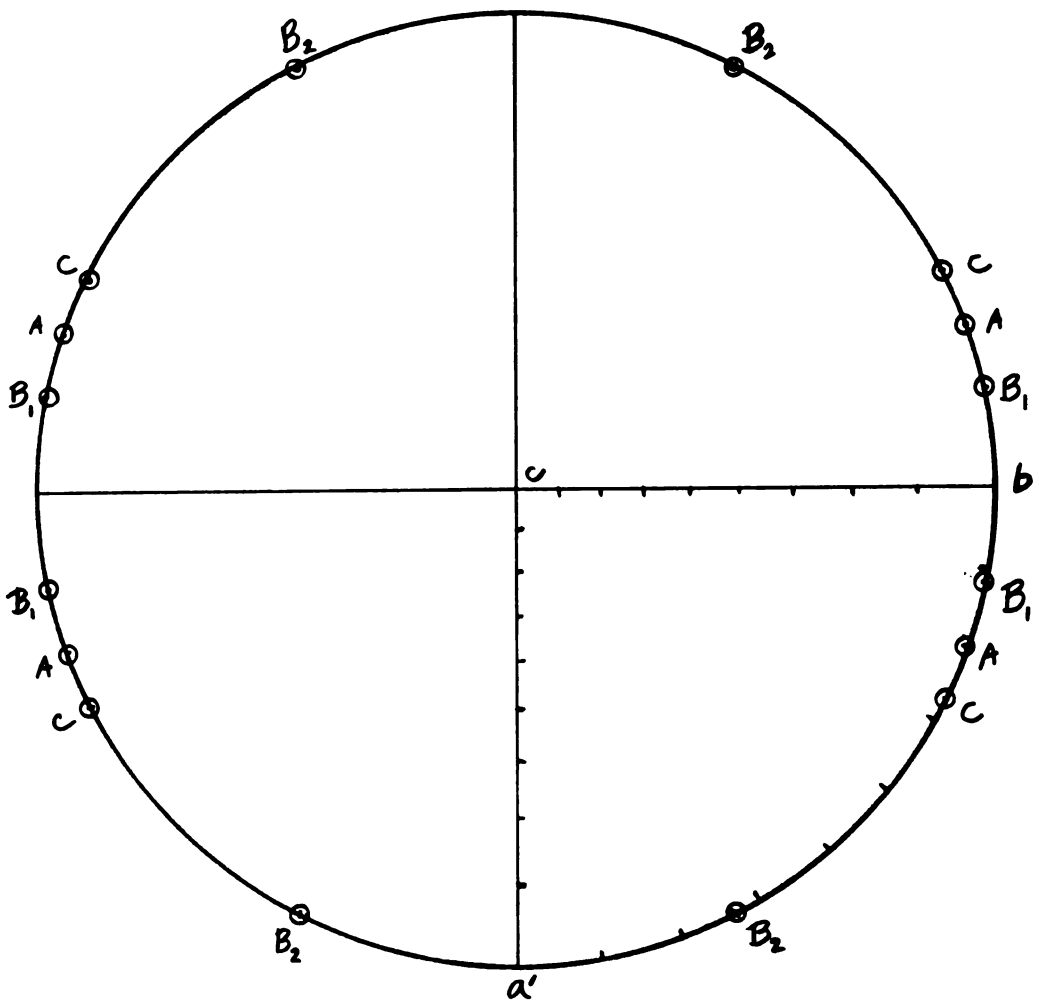

Figure 7. Stereographic projection of the local magnetic fields at the proton sites in $MnCl_2 \cdot 4H_2O$ at 1.17°K.

Fig.A 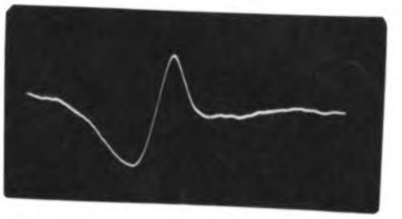

Fig.B 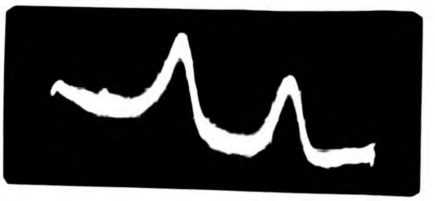

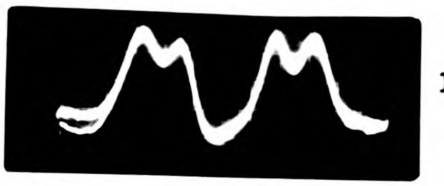 Fig.C

Fig.D 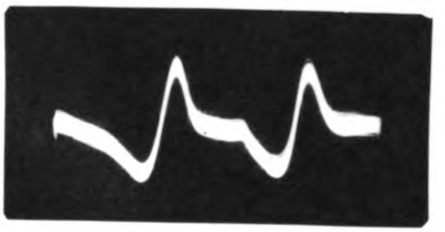

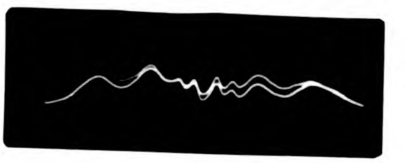 Fig.E

Fig.F 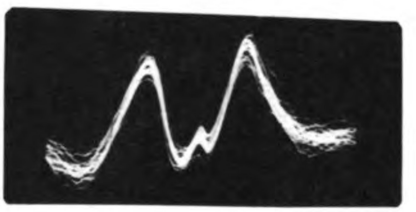

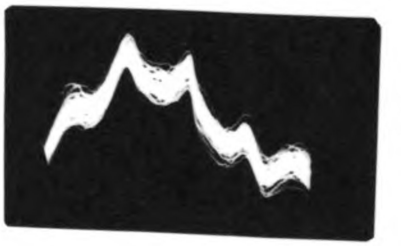 Fig.G

Fig.H 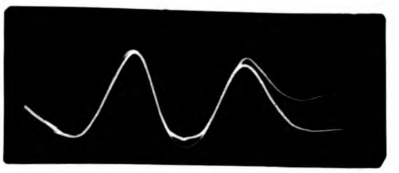

Fig.A to Fig.G : Zero-field signals of proton(s) in crystals in antiferromagnetic state.

Fig.A: A coalesced proton signal in $CoCl_2.6H_2O$.

Fig.B and C: Signals in $NiCl_2.6H_2O$.

Fig.D: of $CoBr_2.6H_2O$.

Fig.E: of $CuCl_2.2H_2O$.

Fig.F and G: of $MnCl_2.4H_2O$.

Fig.H: Zero-field proton signal in $Mn(CH_3COO)_2.4H_2O$ at 2.4° K.

LIST OF REFERENCES

1. Andrew, E. R. Nuclear Magnetic Resonance. Cambridge University Press (1956).

2. Poulis, N. J., Hardeman, G. E. G., Van der Lugt, W., and Hass, W. P. A. Physica, XXIV, 280 (1958).

3. Mizuno, Joji. Jour. of the Phys. Soc. of Japan, Vol. 15, No. 8, 1412 (1959).

4. Mizuno, Joji. Jour. of the Phys. Soc. of Japan, Vol. 16, No. 8, 1574 (1960).